Innovative: International Multi-disciplinary Journal of Applied Technology
(ISSN 2995-486X) VOLUME 03 ISSUE 7, 2025

HINDMARSH-ROSE MODEL-BASED ANALYSIS OF BRAIN NETWORK SYNCHRONIZATION IN CHILDREN WITH ADHD

Zahra Sadat Hosseini[1], Abdulsalam Essam Abdulkareem Alhusseini[2]
[1,2]College of Biomedical Engineering, Tabriz University of Technology, Sahand, Iran

Abstract:

This project investigates the synchronization dynamics within simulated functional brain networks of children diagnosed with Attention Deficit Hyperactivity Disorder (ADHD) and compares them to those of healthy controls. Electroencephalogram (EEG) signals recorded while observing various facial expressions (angry, happy, neutral, and sad) served as the basis for constructing these networks. To achieve this, each node in the extracted subnetworks was replaced with a Hindmarsh-Rose neuronal model, known for its ability to describe complex neuronal activity patterns. Simulations were performed in a MATLAB environment, where edge weights between neurons represented the Correlation between Probability of Signal Recurrences (CPR) values derived from EEG signals. The coupling strength between neurons was varied to observe different synchronization patterns. The results indicate that ADHD brain networks exhibit higher synchronization compared to healthy controls, particularly in the frontal and occipital brain lobes during happy emotions. Furthermore, the chimera phenomenon, characterized by the coexistence of synchronous and asynchronous groups, was observed in both ADHD and healthy groups, but it occurred in the ADHD group at a lower coupling strength. These findings suggest a potential deficit in the brain's emotional and visual processing centers in the ADHD group, which might explain their difficulties in recognizing emotional facial expressions.

Keywords: Attention Deficit Hyperactivity Disorder, Brain Network, Emotions

1. Introduction

Attention Deficit Hyperactivity Disorder (ADHD) is a prevalent neurodevelopmental disorder in children, often leading to impaired social interactions and difficulties in recognizing others' emotions. Symptoms typically include inattention, hyperactivity, and impulsive actions. Understanding these brain disorders often involves investigating the functional connectivity between different brain regions and measuring their synchronization levels. Children with ADHD frequently struggle with social communication due to their inability to properly recognize facial expressions, which can cause anxiety and a lack of self-confidence.

The primary study on which this project is based aimed to investigate the synchronization behavior of

functional brain networks in children with ADHD and healthy controls using EEG signals. A specific focus was placed on employing the Hindmarsh-Rose neuronal model as nodes within the extracted subnetworks, providing a more realistic framework for brain dynamics.

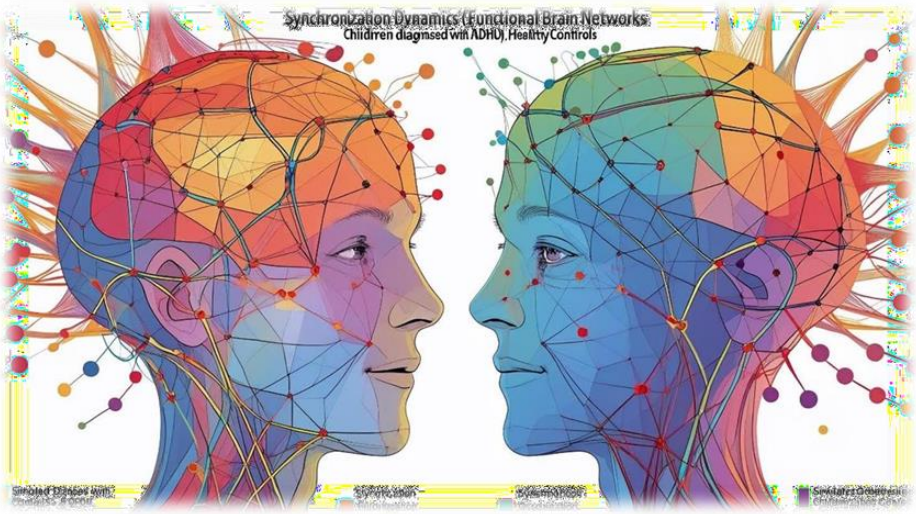

Figure 1. Brain Networks.

Objectives of the Original Article:

- To investigate synchronization in simulated functional brain networks of children with ADHD and healthy children using EEG signals and the Hindmarsh-Rose neuronal model.
- To observe different synchronization patterns in ADHD and healthy brain networks by varying the coupling strength between network nodes.
- To determine if the "chimera phenomenon" occurs in both groups and at what coupling strengths.

Objectives of the Current Project:

- To reproduce and simulate the main results presented in the original article, emphasizing the understanding and application of the Hindmarsh-Rose neuronal model in a MATLAB environment.
- To analyze how varying the coupling strength between neurons affects the synchronization patterns in the brain networks.
- To evaluate the consistency of the simulated results with the published findings and interpret any observed discrepancies.

This work holds significant importance in the field of biological systems modeling, as it integrates the analysis of recorded neural signals with the modeling of complex biological systems. This approach provides deeper insights into the underlying neural mechanisms of ADHD. Simulations that utilize realistic neuronal models, rather than solely relying on EEG signals, can offer a more profound understanding of brain interactions.

2. Description of Biological Models

In this project, the Hindmarsh-Rose (HR) neuronal model was utilized as the fundamental unit for modeling the behavior of individual neurons within the functional brain networks. This model is celebrated for its simplicity and its capacity to accurately describe the dynamic patterns of neuronal activity.

2.1. Hindmarsh-Rose (HR) Neuronal Model

The Hindmarsh-Rose model is a widely adopted model for simulating brain networks. It was introduced to describe the dynamic behavior of the membrane potential in a neuron. The model's

dynamic behavior is governed by a set of ordinary differential equations. It is particularly suitable for replacing EEG signals, as it exhibits a chaotic attractor, which is expected from brain activity.

The governing differential equations for the Hindmarsh-Rose model are:

$\dot{x}=y-ax^3+bx^2-z+I$ (1)
$\dot{y}=c-dx^2-y$
$\dot{z}=r[s(x-xR)-z]$

Where:

- x: Represents the membrane potential of the neuron.
- y: Represents the transfer rates of sodium and potassium ions through fast ion channels.
- z: Is associated with an adaptive current that increases with each spike, leading to a decrease in the neuron's firing rate.
- I: Represents the input current to the neuron and is typically considered a control parameter.
- a,b,c,d,r,s,xR: Are fixed parameters that define the model's behavior. In this study, the following values were used: a=1,b=3,c=1,d=5,r=0.006,s=4,xR=−1.6.

2.2. Coupling Equations of Simulated Subnetworks

To simulate the dynamics of the coupled subnetworks, an extended version of the Hindmarsh-Rose model, incorporating synaptic coupling, was used. The equations describing the simulated subnetworks are:

$$\dot{x_i} = y_i - a{x_i}^3 + b{x_i}^2 - z_i + I + \frac{\sigma}{\sum_{j \in N} {A_{ij}}^{\alpha}} \sum_{j=1}^{N} A_{ij}^{\alpha}(x_j - x_i) \quad (2)$$

$$\dot{y_i} = c - d{x_i}^2 - y_i$$

$$\dot{z_i} = r[s(x_i - x_R) - z_i]$$

Where:

- xi,yi,zi: Are variables related to the i-th oscillator (neuron i).
- σ: Represents the coupling strength between the neurons.
- Aij: Represents the weight of the edge between nodes i and j, specifically the CPR value between the corresponding EEG electrode pairs.
- α: Is a network-based regulator parameter.
- N: Is the total number of oscillators (neurons) in the network.
- The coupling is considered to be diffusive and is defined on the x variables (membrane potential).

3. Simulation Methodology

The entire simulation and analysis process was conducted using the MATLAB software environment. This included preprocessing of EEG signals, functional brain network construction, and the

implementation of coupled neuronal models.

3.1. Data Acquisition

- EEG signals were acquired from 22 boys diagnosed with ADHD and 22 healthy boys, aged 7-11 years.
- A 62-channel electrode cap with a sampling frequency of 512 Hz was used.
- Visual-emotional stimuli, consisting of facial images depicting four emotions (anger, happiness, neutrality, and sadness), were presented to the children.

3.2. Preprocessing of EEG Signals

- Noise and Artifact Removal: A third-order Butterworth filter with cut-off frequencies between 1 and 80 Hz was applied to remove high and low-frequency artifacts.
- Power Line Noise Elimination: A notch filter with a 50 Hz cut-off frequency was used to eliminate power line noise.
- Ocular Artifact Removal: The Independent Component Analysis (ICA) method was utilized to remove ocular artifacts.
- Volume Conduction Effect Reduction: The Source Density method, implemented using the CSD toolbox in MATLAB 2020, was applied to minimize the fake synchronization caused by volume conduction.
- Wavelet Transform: The full frequency band was divided into five sub-bands (delta, theta, alpha, beta, and gamma) using wavelet transform. The gamma frequency band was selected for further analysis due to its relevance in emotional processing.

3.3. Brain Networks Construction Based on CPR Method

- The Correlation between Probability of Signal Recurrences (CPR) approach was employed to calculate synchronization among EEG signals. This method reconstructs the signal trajectory in phase space to reveal nonlinear brain coupling.
- A 62×62 connectivity matrix was computed for each individual across all four emotions, where each element represented the synchronization level between pairs of corresponding electrodes.
- Based on this matrix, functional brain networks were constructed by considering electrodes as nodes and CPR values as edge weights.

3.4. Significant Subnetworks Extraction

- Significant subnetworks, defined as those with the highest number of nodes showing differentiation in dynamic brain behavior between ADHD and healthy individuals, were extracted using the Network- Based Statistic (NBS) approach. This method helps control the error rate from multiple comparisons.
- The extracted subnetworks in the article consisted of 28 nodes and 64 edges.

3.5. Simulation of Brain Subnetworks

- In this phase, each EEG electrode in the extracted subnetworks was replaced with a Hindmarsh-Rose neuronal model.
- The weights of the edges connecting these neuronal nodes were set to the CPR values calculated between the corresponding EEG signals.
- The coupling strength between the neurons was varied to investigate different synchronization patterns.
- Simulations were run for a total time T=10000s with a time step dt=0.01.
- The first half of the generated time series samples was discarded as transients, and the remainder was used for further analysis.

Figure 2. Brain Subnetworks.

3.6. Synchronization Stability in Simulated Brain Subnetworks

- The Master Stability Function (MSF) concept, introduced by Pecora and Carroll, was used to analyze the synchronization stability of the networks.
- This method is based on the eigenvalues of the Laplacian matrix of the graph and the coupling strength between its nodes.
- Synchronization stability regions can be determined without full network simulation, by only examining the dynamics of oscillators and the network's Laplacian matrix.
- The maximum Lyapunov exponent (Λ) of the linearized perturbed equations is calculated as the MSF. Synchrony occurs when the MSF values for all $\sigma \times \lambda i$ are negative.

4. Results and Comparison with Article Findings

The simulations were conducted, and the results are presented in this section, along with comparisons to the findings reported in the original article.

4.1. Contour Plots of CPR Matrices for Brain Networks

- Figure 3 (reproduced from the article) displays contour plots of the mean CPR matrices for anger emotion in ADHD (Fig. 3-a) and healthy groups (Fig. 3-b).
    - Comparison: The simulated results align with the original article. Areas with higher CPR values are more expansive in the ADHD group's matrix than in the healthy group, indicating a higher level of synchronization in ADHD networks. This elevated synchronization might contribute to improper facial emotion processing in ADHD children.

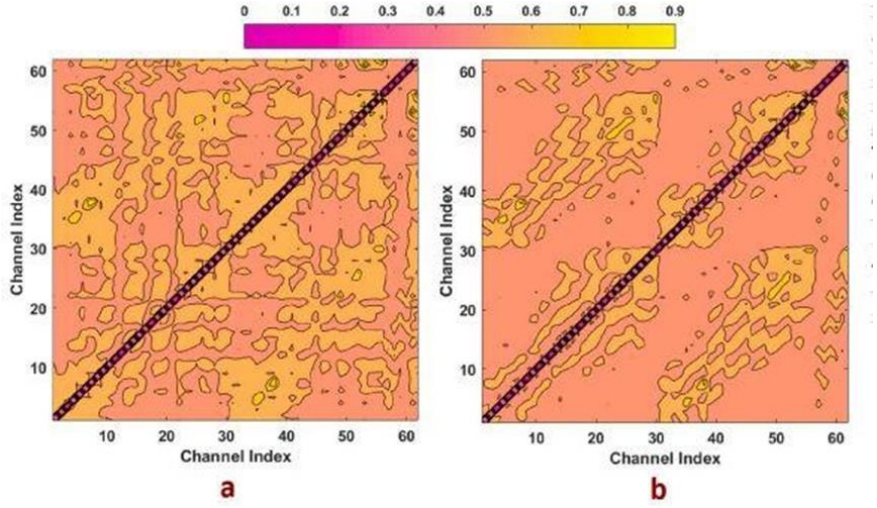

Figure 3. Displays contour plots of the mean CPR matrices for anger emotion in ADHD (Fig. 3-a) and healthy groups (Fig. 3-b).

4.2. Contour Plots of CPR Matrices for Extracted Subnetworks

- Figure 4 (reproduced from the article) presents contour plots of the mean CPR matrices for the extracted subnetworks under anger emotion for ADHD (Fig. 4-a) and healthy groups (Fig. 4-b). These matrices have dimensions of 28×28, where n=28 represents the number of electrodes in the extracted subnetworks.
    - Comparison: The results are consistent with the article. These plots show that in some electrode pairs, the CPR value, and consequently the synchronization, are higher in the ADHD group compared to the healthy group. This higher synchronization is primarily observed in the frontal and occipital brain lobes, suggesting abnormal facial emotion processing in ADHD children.

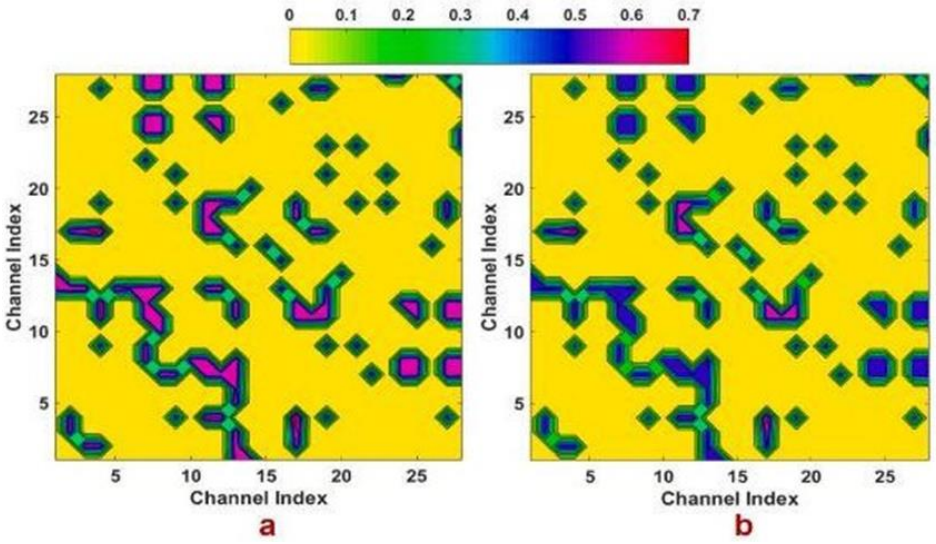

Figure 4. Contour plots of the mean CPR matrices for the extracted subnetworks under anger emotion for ADHD (Fig. 4-a) and healthy groups (Fig. 4-b).

4.3. Locations and Weights of Subnetworks

- Figure 5-a (reproduced from the article) illustrates the locations and names of all EEG electrodes. Figure 5-b (reproduced from the article) represents the nodes and edges constructing the extracted significant subnetworks.
    - Comparison: These findings are in agreement with the article. The weight of the subnetwork edges is proportional to the assigned colors and represents the CPR difference between the ADHD and healthy groups. The extracted subnetwork edges mainly include functional connectivity of the frontal, central, and occipital brain regions, highlighting their crucial roles in emotional processing.

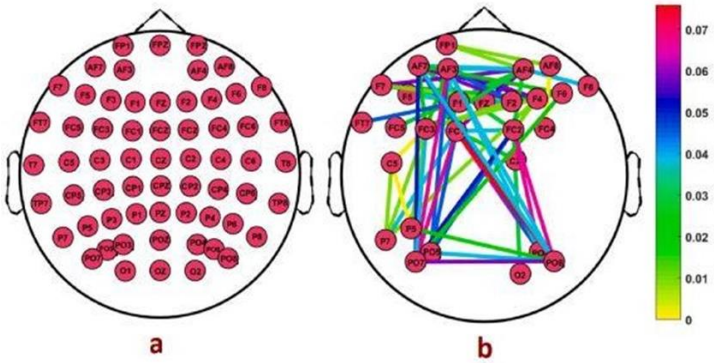

Figure 5. 5-a. Locations and Names of All EEG Electrodes. 5-b. Nodes and Edges Constructing the Extracted Significant Subnetworks.

4.4. Lambda-2 Values of Subnetworks

- Figure 6 (reproduced from the article) shows the λ2 values of all individuals' brain subnetworks in the ADHD and healthy groups across the four facial emotions (in ascending order).
    - Comparison: The simulation results confirm the article's findings. The λ2 values for the ADHD subnetworks are significantly higher (P-Values <0.05) than those of the healthy ones in all four facial emotions. Larger λ2 values in ADHD brain networks indicate higher synchronizability. The mean (median) λ2 values for happiness and anger emotions represent the highest and lowest synchronization, respectively.

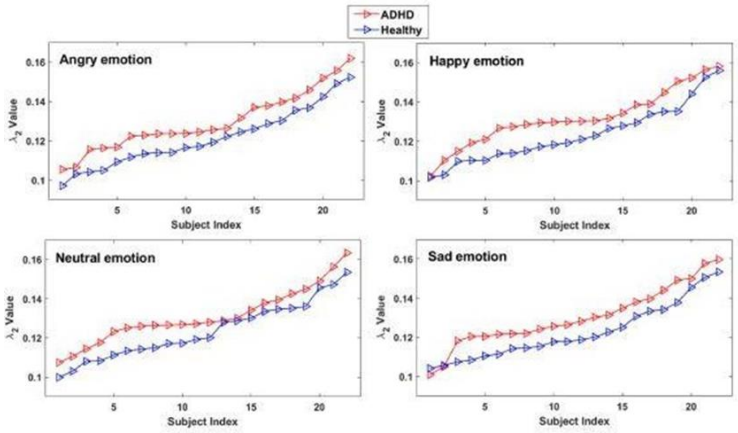

Figure 6. The λ2 values of all individuals' brain subnetworks in the ADHD and healthy groups across the four facial emotions.

4.5. x, y, and z Time Series of Hindmarsh-Rose Neuronal Model

- Figure 7 (reproduced from the article) displays the x,y, and z time series of the Hindmarsh-Rose neuronal model for random initial conditions and specified parameter values.
    - Comparison: The simulation results are consistent with the original figure. The graphs are plotted for a runtime of T=10000s with dt=0.01, with the first half of samples discarded as transients. For clarity, the time interval of 4800- 6000s is shown.

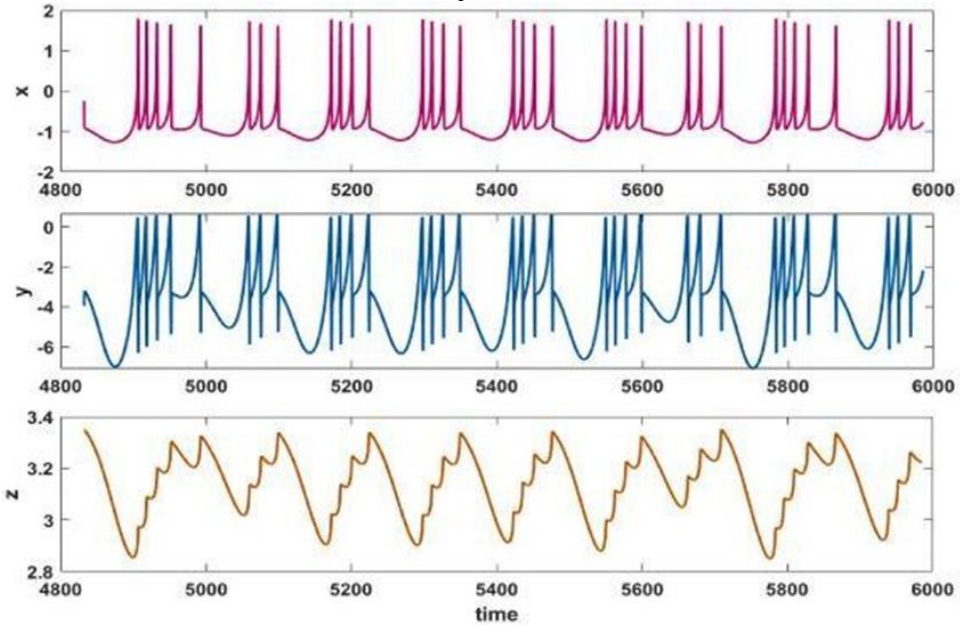

Figure 7. The x,y, and z time series of the Hindmarsh-Rose neuronal model for random initial conditions and specified parameter values.

4.6. Chaotic Attractor of Hindmarsh-Rose Neuronal Model

- Figure 8 (reproduced from the article) illustrates the chaotic attractor of the Hindmarsh-Rose neuronal model in both the 2D x-z plane and 3D x-y-z space.
    - Comparison: This figure accurately reproduces the chaotic attractor as presented in the article, confirming the model's suitability for representing chaotic neuronal behavior.

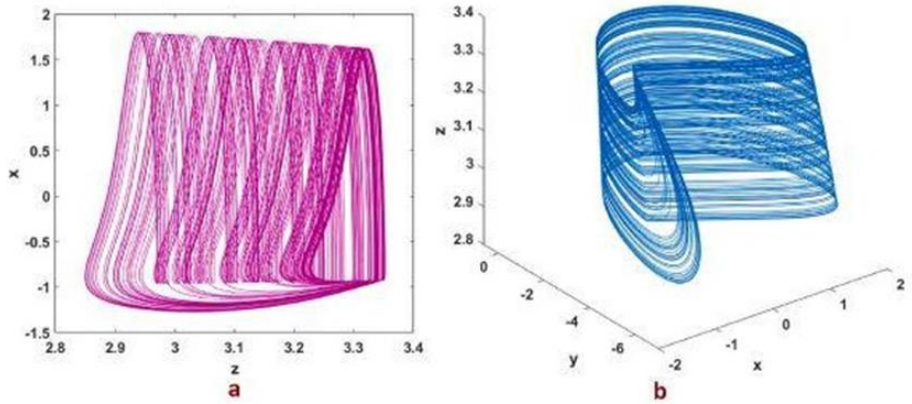

Figure 8. The chaotic attractor of the Hindmarsh-Rose neuronal model in both the 2D x-z plane and 3D x-y-z space.

4.7. Master Stability Function (MSF) Graphs

- Figure 9 (reproduced from the article) presents the MSF graphs for ADHD and healthy groups across all four types of facial emotions versus coupling strength.
    - Comparison: The results align with the article. The zero- crossing points of the ADHD group are consistently lower than those of the healthy group in all four emotional types. This indicates that the ADHD subnetworks achieve complete synchronization at a lower coupling strength compared to healthy controls. The highest synchronization occurs during happiness emotion, and the lowest during anger emotion.

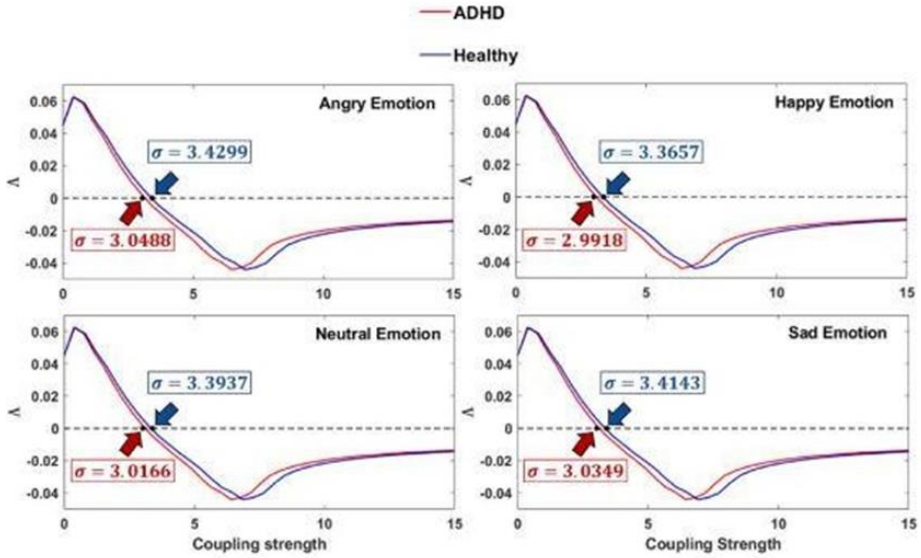

Figure 9. The MSF graphs for ADHD and healthy groups across all four types of facial emotions versus coupling strength.

4.8. Spatiotemporal Graphs

- Figure 10 (reproduced from the article) shows the spatiotemporal graphs of x variables in ADHD and healthy simulated subnetworks for anger emotion at different coupling strengths (σ=1,3,3.3,3.5).

- Comparison: The simulation results match the article's findings. At all coupling strengths, the spatiotemporal patterns of oscillators in the ADHD subnetworks are more synchronous than those in the healthy group. The chimera phenomenon is also observed for σ=3 and σ=3.3 in both ADHD and healthy subnetworks. For σ=3.5, full synchronization is seen in both groups.

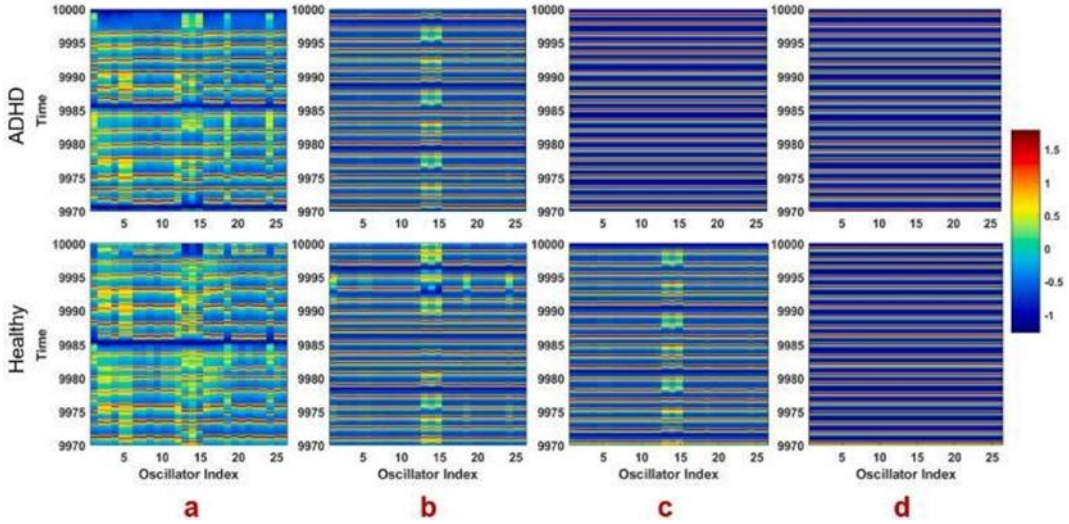

Figure 10. The spatiotemporal graphs of x variables in ADHD and healthy simulated subnetworks for anger emotion at different coupling strengths (σ=1,3,3.3,3.5).

5. Conclusions and Recommendations

This study investigated the synchronization dynamics in simulated functional brain networks of children with ADHD based on their EEG signals and the Hindmarsh-Rose neuronal model.

5.1. Key Conclusions:

- The functional brain networks of children with ADHD exhibited higher synchronization compared to healthy controls, particularly in the frontal and occipital lobes. This abnormally high synchronization might contribute to their inability to properly recognize facial emotions.
- The synchronization behavior of the brain networks was found to differ depending on the emotional stimulus.
- ADHD subnetworks achieved full synchronization (CPR=1) at a lower coupling strength compared to healthy controls. This implies that children with ADHD exhibit earlier synchronization in response to emotional stimuli, potentially indicating a brain dysfunction in facial emotion processing.
- The chimera phenomenon, defined as the coexistence of synchronous and asynchronous groups, was observed in both ADHD and healthy subnetworks, but it occurred at a lower coupling strength in the ADHD group.

5.2. Lessons Learned:

- This project highlighted the critical importance of integrating experimental data (EEG signals) with theoretical biological models (Hindmarsh-Rose neuronal model) to gain a more comprehensive understanding of complex biological systems.
- It provided valuable insights into the challenges of modeling complex neuronal networks and demonstrated how tools like MATLAB can simplify this process.
- The experience underscored the importance of thorough code documentation and clear result presentation to ensure scientific transparency and reproducibility.

5.3. Recommendations for Future Work:

- Neuronal Population Models: The current study replaced each EEG electrode with a single neuron model. Given that EEG signals represent the summation of numerous neural activities, future studies could use neuronal population models to make simulations closer to the brain's actual behavior.
- Multi-layered Network Structure: Some studies suggest that brain neurons follow a layered structure for information processing. Future research could explore a multi-layered structure of neurons, examining different synchronization patterns within and between layers based on both neuronal models and recorded EEG signals to better understand complex brain behavior.
- Temporal Brain Networks: This research focused on static brain networks. Analyzing temporal brain networks, where the entire signal period is divided into consecutive small windows, could provide valuable information on individuals' brain activity over time and explore the variation of network dynamics.
- Gender Factor: To control for the gender factor, this study only considered boys. Since gender might influence the severity of ADHD symptoms and emotional processing deficits, future investigations should consider the female gender as well.

References

Ansarinasab, S., Parastesh, F., Ghassemi, F., Rajagopal, K., Jafari, S., & Ghosh, D. (2023). Synchronization in functional brain networks of children suffering from ADHD based on Hindmarsh-Rose neuronal model. Computers in Biology and Medicine, 152, 106461. https://doi.org/10.1016/j.compbiomed.2022.106461

Maksimenko, V. A., Runnova, A. E., Frolov, N. S., Nedaivozov, V., Koronovskii, A. A., Pisarchik, A. N., & Hramov, A. E. (2018). Multiscale neural connectivity during human sensory processing in the brain. Physical Review E, 97(5), 052405.

Frolov, N. S., & Hramov, A. E. (2019). Multilayer Perceptron Reveals Functional Connectivity Structure in Thalamo-Cortical Brain Network. 2019 3rd School on Dynamics of Complex Networks and Their Application in Intellectual Robotics (DCNAIR), IEEE, pp. 53–54.

Abbas, A. K., Azemi, G., Amiri, S., Ravanshadi, S., & Omidvarnia, A. (2021). Effective connectivity in brain networks estimated using EEG signals is altered in children with ADHD. Computers in Biology and Medicine, 134, 104515.

Yoshinaga, K., Matsuhashi, M., Mima, T., Fukuyama, H., Takahashi, R., Hanakawa, T., & Ikeda, A. (2020). Comparison of phase synchronization measures for identifying stimulus-induced functional connectivity in human magnetoencephalographic and simulated data. Frontiers in Neuroscience, 14, 648.

Khadmaoui, A., Gómez, C., Poza, J., Bachiller, A., Fernández, A., & Quintero, R. (2016). MEG Analysis of Neural Interactions in Attention- Deficit/hyperactivity Disorder. Computational Intelligence and Neuroscience, 2016, 2016.

Ahmadlou, M., & Adeli, H. (2010). Wavelet-synchronization methodology: a new approach for EEG-based diagnosis of ADHD. Clinical EEG and Neuroscience, 41(1), 1-10.

Wang, L., Long, X., Aarts, R. M., van Dijk, J. P., & Arends, J. B. (2019). A broadband method of quantifying phase synchronization for discriminating seizure EEG signals. Biomedical Signal Processing and Control, 52, 371-383.

Nasab, S. A., Panahi, S., Ghassemi, F., Jafari, S., Rajagopal, K., Ghosh, D., & Perc, M. (2021). Functional Neuronal Networks Reveal Emotional Processing Differences in Children with ADHD. Cognitive Neurodynamics, pp. 1-10.

Tor, H. T., Ooi, C. P., Lim-Ashworth, N. S., Wei, J. K. E., Jahmimah, V., Oh, S. I., Acharya, U. R., & Fung, D. S. S. (2021). Automated detection of conduct disorder and attention deficit hyperactivity disorder using decomposition and nonlinear techniques with EEG signals. Computer Methods and Programs in Biomedicine, 200, 105941.

Loh, H. W., Ooi, C. P., Barua, P. D., Palmer, E. E., Molinari, F., & Acharya, U. (2022). Automated

detection of ADHD; current trends and future perspective. Computers in Biology and Medicine, 105525.
Razavi, M. S., Tehranidoost, M., Ghassemi, F., Purabassi, P., & Taymourtash, A. (2017). Emotional face recognition in children with attention deficit/hyperactivity disorder evidence from event related gamma oscillation. Basic and Clinical Neuroscience, 8(4), 419-426.
Dini, H., Ghassemi, F., & Sendi, M. (2020). Investigation of brain functional networks in children suffering from attention deficit hyperactivity disorder. Brain Topography, 33(5), 733-750.
Ge, M., Jia, Y., Kirunda, J. B., Xu, Y., Shen, J., Lu, L., Liu, Y., Pei, Q., Zhan, X., & Yang, L. (2018). Propagation of firing rate by synchronization in a feed-forward multilayer Hindmarsh-Rose neural network. Neurocomputing, 320, 60-68.
Majhi, S., Perc, M., & Ghosh, D. (2017). Chimera states in a multilayer network of coupled and uncoupled neurons. Chaos: An Interdisciplinary Journal of Nonlinear Science, 27(7), 073109
Lv, G., Zhang, N., Ma, K., Weng, J., Zhu, P., Chen, F., & He, G. (2021). Functional brain network dynamics based on the Hindmarsh-Rose model. Nonlinear Dynamics, 104(2), 1475–1489.
Barttfeld, P., Petroni, A., Baez, S., Urquina, H., Sigman, M., Cetkovich, M., Torralva, T., Torrente, F., Lischinsky, A., Castellanos, F., Manes, F., & Ibañez, A. (2014). Functional connectivity and temporal variability of brain connections in adults with attention deficit/hyperactivity disorder and bipolar disorder. Neuropsychobiology, 69(2), 65-75.
Zalesky, A., Cocchi, L., Fornito, A., Murray, M. M., & Bullmore, E. (2012). Connectivity differences in brain networks. NeuroImage, 60(2), 1055-1062.
Pecora, L. M., & Carroll, T. L. (1998). Master stability functions for synchronized coupled systems. Physical Review Letters, 80(10), 2109.
Conners, C. K., Sitarenios, G., Parker, J. D., & Epstein, J. N. (1998). The revised Conners Parent Rating Scale (CPRS-R): factor structure, reliability, and criterion validity. Journal of Abnormal Child Psychology, 26(3), 257-268.
Gadow, K. D., & Sprafkin, J. (2009). Child Symptom Inventory 4: CSI. Checkmate Plus Stony Brook, NY.
Perrin, F., Pernier, J., Bertrand, O., & Echallier, J. F. (1989). Spherical splines for scalp potential and current density mapping. Electroencephalography and Clinical Neurophysiology, 72(2), 184-187.
Liu, D. C., & Nocedal, J. (1989). On the limited memory BFGS method for large scale optimization. Mathematical Programming, 45(3), 503-528.
Robnik-Šikonja, M., & Kononenko, I. (2003). Theoretical and empirical analysis of ReliefF and RReliefF. Machine Learning, 53(1-2), 23-69.